









Research Article

Comparative Analysis of a Super-Wideband Millimeter Wave Array Antenna for Body-Centric Communications

Abdullah G. Alharbi ¹, **Mohammad Monirujjaman Khan** ², **Kaisarul Islam** ²,
Md. Nakib Alam Shovon,² **Mohammad Inam Abbasi** ³, **Sami Bourouis** ⁴,
Hany S. Hussein ^{5,6}, **Hammam Alshazly** ⁷, and **Thabet Slimani** ⁸

¹Department of Electrical Engineering, Faculty of Engineering, Jouf University, Sakaka 42421, Saudi Arabia

²Department of Electrical and Computer Engineering, North South University, Dhaka-1229, Bangladesh

³Centre for Telecommunication Research & Innovation (CETRI),

Faculty of Electrical and Electronic Engineering Technology (FTKEE), Melaka (UTeM), Melaka 76100, Malaysia

⁴Department of Information Technology, College of Computers and Information Technology, Taif University, P.O. Box 11099, Taif 21944, Saudi Arabia

⁵Electrical Engineering Department, Faculty of Engineering, King Khalid University, Abha 62529, Saudi Arabia

⁶Electrical Engineering Department, Faculty of Engineering, Aswan University, Aswan 81528, Egypt

⁷Faculty of Computers and Information, South Valley University, Qena 83523, Egypt

⁸Applied College, Department of Technology, Taif University, P.O. Box 11099, Taif 21944, Saudi Arabia

Correspondence should be addressed to Mohammad Monirujjaman Khan; monirujjaman.khan@northsouth.edu

Received 27 October 2021; Accepted 22 February 2022; Published 18 March 2022

Academic Editor: Eng Hock Lim

Copyright © 2022 Abdullah G. Alharbi et al. This is an open access article distributed under the Creative Commons Attribution License, which permits unrestricted use, distribution, and reproduction in any medium, provided the original work is properly cited.

The future of wireless technology is moving towards millimeter wave bands due to a surge in the use of wearable gadgets in current wireless bands. The 60 GHz band is unlicensed around the world and has gathered high research interest. At this band, the atmospheric absorption is very high, which results in short-range communication. High gain antennas are a core requirement for operating at 60 GHz. In this paper, we are proposing three different arrays consisting of 2, 3, and 4 elements of a novel patch design. The radiating patch consists of a semicircular disc fed by a microstrip feed line. The ground plane has been etched into a novel shape. The radiator and the ground plane are attached to a 1.5 mm thick FR-4 substrate which has a relative permittivity of 4.3. The radiating elements are connected linearly to form arrays. In free space, all three arrays achieved a very wide bandwidth of more than 20 GHz, and the maximum gain varied from 3.44 dBi to 6.2 dBi. The arrays were also simulated under human body conditions by modelling a three-layer phantom. At different distances from the phantom, the maximum gain increased by more than 1 dBi. The antenna shows 4.855 dBi, 5.032 dBi, and 6.66 dBi gain for 2 array, 3 array, and 4 array, respectively, when simulated on the three-layer human model phantom. The antenna has a very good VSWR value for all three array structures. On the human body phantom, the proposed antenna design in this research shows 1.214, 1.120, and 1.023 VSWR values for 2 array, 3 array, and 4 array, respectively. The efficiencies were highly affected, as expected from patch antennas. The simulation results are obtained from CST Microwave Studio.

1. Introduction

Demand for high data rates and the usage of smart devices has increased exponentially in the last few decades. To avoid interference and overburdening of current microwave

systems, millimeter wave (mmWave) is fast becoming the preferred range of communications. The 60 GHz band of the mmWave has a bandwidth of more than 7 GHz and is suitable for short-ranged indoor applications. The band is unlicensed in different countries, which makes it very

promising. High data rates of more than 7 Gbps can be achieved with low interference and a high level of security [1–4]. At 60 GHz, the atmospheric absorption is very high and, along with propagation losses, the range of mmWave is very short. On the other hand, this property gives high security as it becomes very difficult for other neighboring networks to interfere with signals. Until now, the 60 GHz band was exclusively available for noncommercial applications like the military and satellites [5]. The unlicensed 60 GHz band is gathering a lot of interest from researchers who are focused on developing systems such as healthcare and multimedia. In systems like health care, the nodes are connected around the human body. The networking between these nodes is known as a wide-body area network or WBAN. Antennas for WBANs must be tiny and flexible, and appropriate radiation patterns must be considered based on the position of the node. Furthermore, the human body's influence on the performance of the antenna should also be studied [6, 7].

From link budget analysis, it can be concluded that a high gain antenna is a core requirement for the 60 GHz band after considering several factors such as distance, power constraint, and bandwidth. [8]. A disc-shaped antenna with 5.2 dB gain is proposed in [9]. A wearable textile antenna with 11.9 dBi gain for WBAN applications is presented by Chahat et al. [10]. A compact novel design and a comparative analysis of a 60 GHz antenna are presented in [11, 12] for body-centric applications that achieve a maximum gain of 9.73 dB to 10 dB. To raise the gain even further, antennas can be arranged in linear or planar arrays. Zhan et al. presented two different 60 GHz patch arrays in [13]. The first design is a 4×1 linear array, and the second design is a 4×4 planar array. The linear array achieved a bandwidth of 10 GHz with a maximum gain of 12.5 dBi. In comparison, the planar array achieved a slightly lower bandwidth, but the maximum gain increased to 18 dBi. Two Yagi array designs with two and four elements are presented in [14]. The 4-element array achieved a bandwidth of 8.2 GHz with a maximum gain of 13.85 dBi and an efficiency of 95.4%. A 7×7 phased array antenna with a gain of 22.15 dBi is presented in [15]. Four different array configurations have been proposed in [16]. The maximum gain varied in the range of 12.8 to 15.6 dBi. Hong and Choi explored a 4-port array design under human phantom conditions in [17]. Wu et al. developed an E-shaped patch array for the 60 GHz band that achieved a maximum gain of 17.92 dBi [8]. The gain of a four-element patch array based on a cotton textile substrate was 12.6 dBi [18]. The same design was studied on a RT 5880 substrate in [19] with a 3 mm thick ground plane in order to achieve a low SAR value. Compared to a single patch, the array configuration achieved a 5 dBi higher maximum gain. Leduc and Zhadobov in their paper proposed three different feeding techniques for the four-element patch array to reduce radiation exposure to the human body [20]. Two different Yagi designs were presented in [21] in order to achieve a wide bandwidth and high gain. The conventional Yagi design achieved a high gain of 17 dB with a bandwidth of 6 GHz, while the SIW Yagi achieved a bandwidth of 7 GHz with a slightly lower gain of 15 dB. A T shape

mmWave array antenna for 5 G system is proposed in [22]. The antenna is designed on a Rogers substrate with a dielectric constant of 2.3. It works at 28 GHz with an impedance bandwidth of 8 GHz. The overall size of the antenna presented in [22] is $25 \text{ mm} \times 18.85 \text{ mm}$. A 60 GHz mmWave antenna designed on different textile substrates is presented in [23]. The antenna was proposed for wearable application, and its on-body performance was investigated. It was designed on a 100 percent polyester substrate at first and afterwards on several textile substrates. The antenna's overall dimensions are 12.2 mm by 12 mm, and it operates at 60 GHz with an 11.632 GHz impedance bandwidth [23]. A Q-slot antenna for on-body applications is given in [24]. It operates at 60 GHz. The antenna is printed on the substrate with an overall size of $12.9 \text{ mm} \times 14 \text{ mm}$. The antenna presented in [24] has an impedance bandwidth of 12.11 GHz.

In this paper, we are proposing three different array configurations of a novel microstrip patch antenna design. The aim is to achieve a super wide bandwidth and a high gain. As reported in [21], a compromise is needed between bandwidth and gain. Our goal is to achieve a bandwidth of more than 20 GHz with a sufficient amount of gain for short transmissions. The patch elements are arranged in 2, 3, and 4 array configurations. Each configuration is studied under human conditions by considering a three-layer phantom. The paper is divided into five sections. The three array designs are laid out in Section 2. The third section consists of free-space simulation results. Section four contains the findings of the on-body simulation, and Section 5 contains the conclusion. The design and simulations were done using CST Microwave Studio.

2. Antenna Design

Each single element of the three arrays consists of a semi-circular disc patch. The ground plane has a novel shaped slot etched into it that is complementary to the radiating patch. All three antenna arrays are designed on a 1.5 mm thick FR-4 substrate which has a relative permittivity of 4.3. The radiating patches are made from 0.035 mm thick PEC. The material thicknesses are presented in Table 1.

The first of the three proposed array designs is a two-element array (Array 2), presented in Figure 1. A 2.5 mm long, 0.7-width microstrip line feeds the patches, which are 9.5 mm apart. The ground plane is 2.5 mm apart. The detailed dimensions of Array 2 are marked in Figure 1, and the values are given in Table 2. The Array 3 design consists of three patches (Figure 2). The middle patch and the right side patch are facing each other and are the same distance apart as Array 2. The left side element is 8.1 mm away and is facing in the opposite direction to the middle patch. The detailed dimensions of Array 3 are given in Table 3. Similarly, for Array 4, one more element is added 8.1 mm away to the right side of Array 3 and is facing in the opposite direction. The dimensions are detailed in Figure 3 and Table 4. The antenna's wavelength at 60 GHz is 5 mm. The electrical size of the length and width of the substrate of a two-array antenna is 0.5λ and 0.3λ , respectively. The electrical size of the length

TABLE 1: Antenna materials and thickness.

Antenna components	Thickness (mm)	Material	Relative permittivity
Ground plane	0.035	PEC	—
Substrate	1.5	FR4	4.3
Radiator	0.035	PEC	—

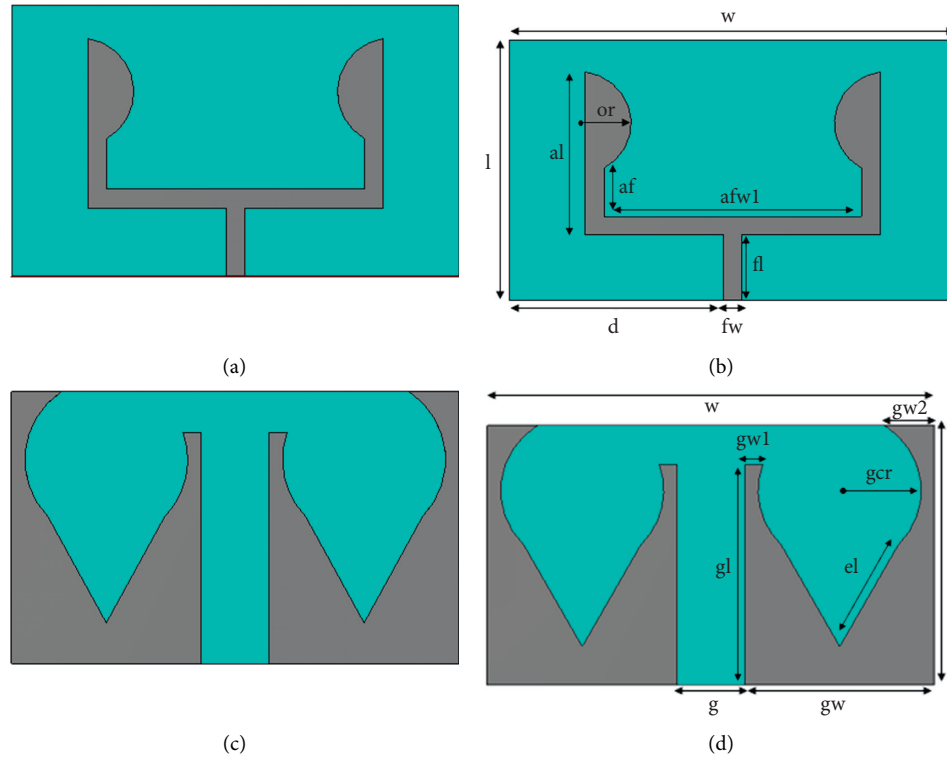


FIGURE 1: Array two (a, b) top view and (c, d) bottom view.(a) View from the top.(b) Top view (schematic diagram).(c) Back view.(d) Back view (schematic diagram).

TABLE 2: Array parameter two dimensions.

S. No.	Parameter	Value (mm)
1	w	16.5
2	l	10
3	or	2
4	af	1.87
5	d	7.9
6	$afw1$	9.5
7	gcr	3
8	$gw1$	0.67
9	gl	8.5
10	fw	0.7
11	fl	2.5
12	al	6.28
13	$gw2$	1.84
14	el	4.46
15	g	2.5
16	gw	7

and width of the substrate of a three-array antenna is 0.5λ and 0.19λ , respectively. Similarly, the electrical size of the length and width of the substrate of a four-array antenna is 0.5λ and 0.14λ , respectively.

3. Free-Space Simulation Results

All three array antennas achieved a very wide bandwidth. The return loss magnitude was less than 10 dB for more than 20 GHz, which covers beyond the unlicensed 60 GHz band. At 60 GHz, the return loss magnitude improved as the number of antenna array elements increased. The return loss curves are depicted in Figures 4–6 for Array 2, Array 3, and Array 4, respectively. The comparison return loss curve is depicted in Figure 7. For all three arrays, the VSWR is less than the acceptable value of 1.5 over the whole simulated range. The individual VSWR is depicted in Figures 8–10, and the comparison is in Figure 11. The H-plane radiation pattern at 60 GHz for Array 2 is omnidirectional, while the E-plane demonstrates a grating pattern (Figure 12). For Array 3, the patterns are more directional, as seen in Figure 13. Array 4 shows even more grating patterns (Figure 14). The gap distance between the antenna elements is responsible for this grating pattern. The polar plot comparisons in Figure 15 and the 3D radiation patterns of the three designs are presented in Figure 16. The maximum gain is 3.44, 4.92, and 6.19 dBi for arrays 2, 3, and 4, respectively. The radiation efficiency is quite low at 41.51% for Array 2. Array 3 achieved

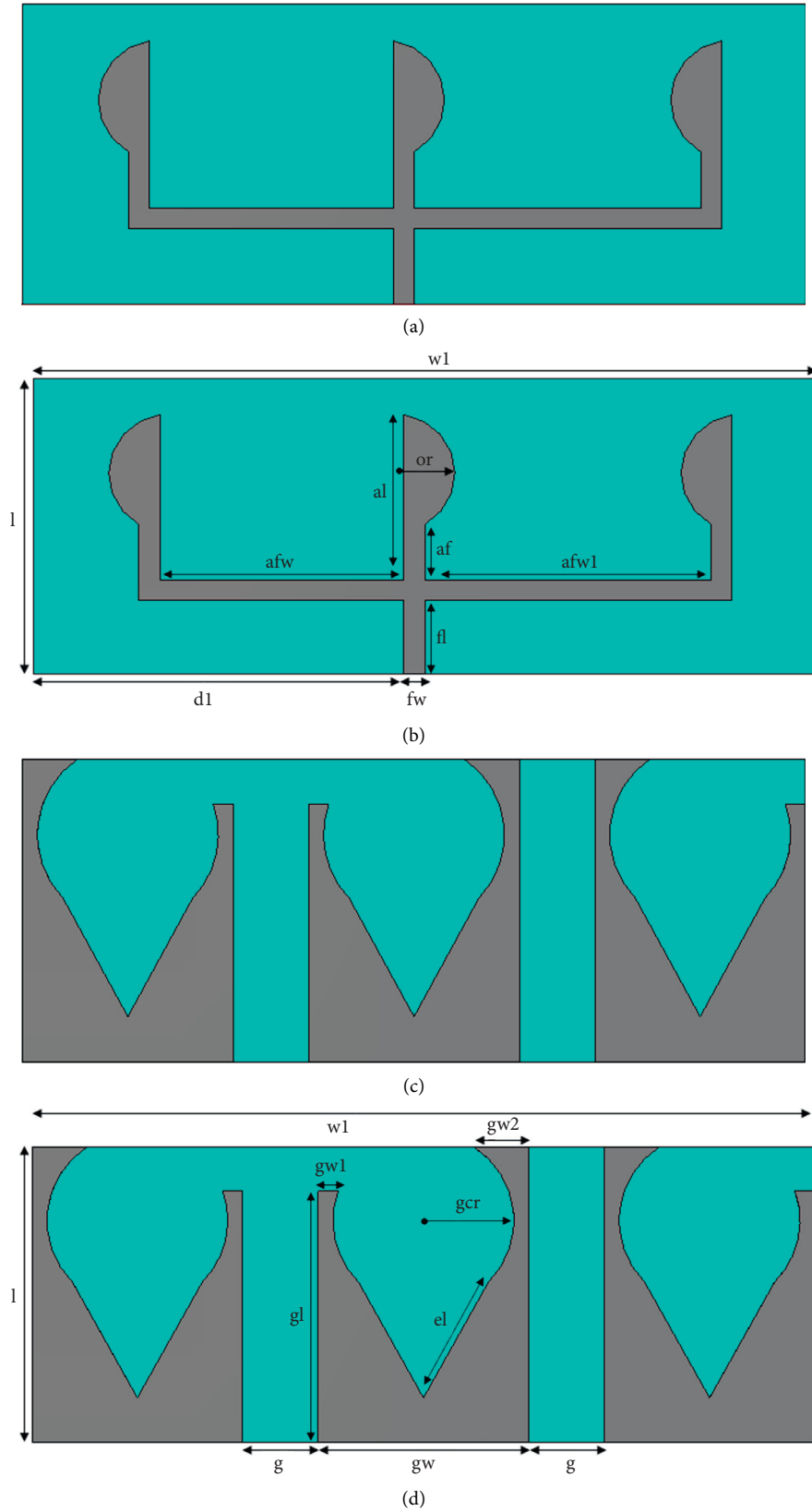


FIGURE 2: Array three (a, b) top view and (c, d) bottom view.(a) View from the top.(b) Top view (schematic diagram).(c) Back view.(d) Back view (schematic diagram).

TABLE 3: Array 3 dimensions.

S. No.	Parameter	Value (mm)
1	w1	26
2	l	10
3	or	2
4	af	1.87
5	d1	12.3
6	afw1	9.5
7	gcr	3
8	gw1	0.67
9	gl	8.5
10	fw	0.7
11	fl	2.5
12	al	6.28
13	gw2	1.84
14	el	4.46
15	g	2.5
16	gw	7
17	afw	8.1

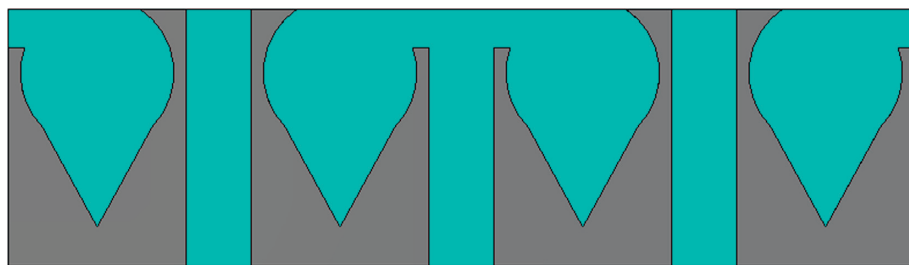
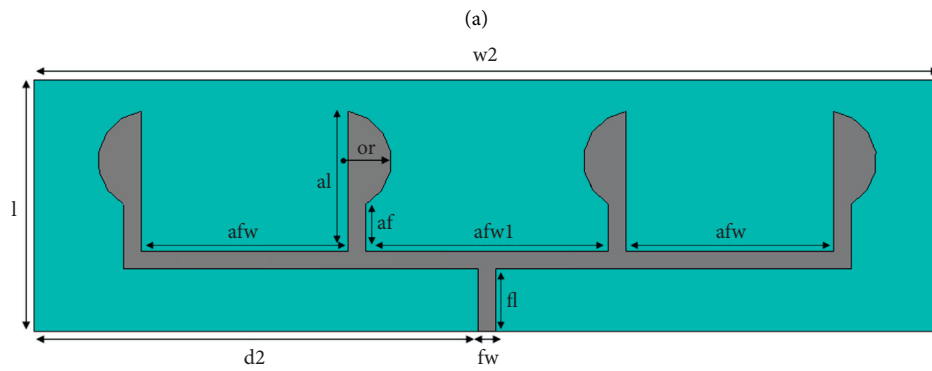
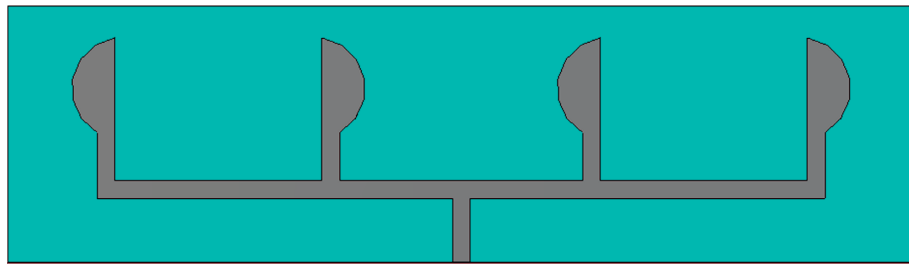


FIGURE 3: Continued.

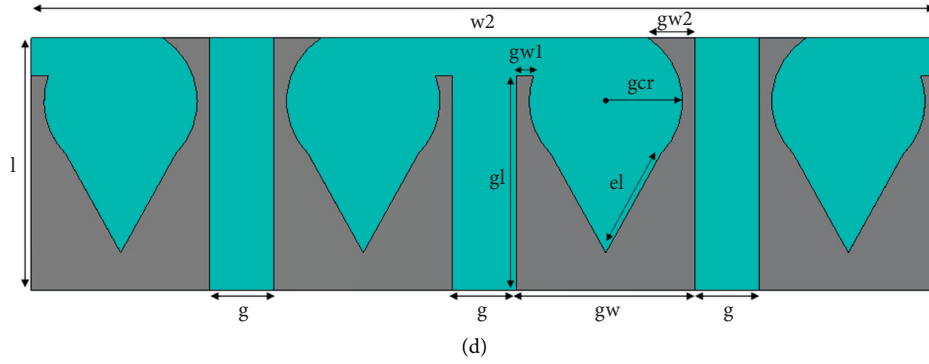


FIGURE 3: Array four (a, b) top view and (c, d) bottom view.(a) View from the top. (b) Front view (schematic diagram). (c) Back view. (d) Back view (schematic diagram).

TABLE 4: Array 4 dimensions.

S. No.	Parameter	Value (mm)
1	w_2	35.5
2	l	10
3	or	2
4	af	1.87
5	d_2	17.47
6	afw_1	9.5
7	g_{cr}	3
8	g_{w1}	0.67
9	gl	8.5
10	fw	0.7
11	fl	2.5
12	al	6.28
13	g_{w2}	1.84
14	el	4.46
15	g	2.5
16	g_w	7
17	afw	8.1

the lowest efficiency. The surface current distributions for all three antennas are depicted in Figure 17. The free-space simulation results are summarized in Table 5.

4. On-Body Simulation Results

Due to the absorption of electromagnetic waves, the antenna's performance is greatly affected by the human body. The radiation pattern gets distorted, and parameters such as efficiency, gain, and return loss are changed. A human torso is built to have the three outermost layers of a human body—skin, fat, and muscle—to replicate an on-body scenario (Figure 18). Table 6 shows the thickness, relative permittivity, and conductivity for these layers at 60 GHz [22]. Depending on the array configuration, the size of the phantom is changed to accommodate the antenna design (Figure 19 and Table 7). For every configuration, the thickness of the three layers is kept constant. For on-body analysis, all three antennas are placed at five different positions away from the phantom at 2 mm intervals (Figure 20).

The return loss curve of Array 2 shifted to the left at different distances from the phantom (Figure 21). The shape

of the curve at different distances remained comparable to free space. A similar pattern is observed for the VSWR (Figure 22). The radiation pattern shows reduced back radiation and grating lobes towards the phantom. The patterns are more grating in the E-plane, whereas the H-plane is comparable to the free space at all distances. The patterns are depicted in Figure 23, and the 3D radiation pattern in Figure 24. Maximum gain was highest at 6 mm away from the phantom. At every other distance, the gain was higher than free space, except at the closest distance from the phantom. The radiation efficiency and the total efficiency decreased by a significant margin, especially at the closest distance to the phantom. These values improved as the gap distance increased gradually. The on-body performance details of Array 2 are summarized in Table 8.

At 8 mm away from the phantom, Array 3 had a similar return loss to free space. The resonant frequencies were closer to free space at this distance. The overall shape of the curves is very similar to the free space (Figure 25). The corresponding VSWR is depicted in Figure 26. The maximum gain improved to more than 5 dBi at 6 mm away from the phantom. At greater distances, the gain was closer to 5 dBi. The radiation patterns at different distances for Array 3 are depicted in Figure 27 and the 3D pattern in Figure 28. The return loss curve of Array 4 reveals that the antenna was resonant extremely close to 60 GHz when it was 6 mm away from the phantom (Figure 29). The VSWR curve shows that at around 60 GHz, the value was very close to 1 (Figure 30). The radiation patterns depicted in Figures 31 and 32 show similarities with the free space patterns at greater distances from the phantom. The detailed on-body performance values are summarized in Tables 9 and 10 for Arrays 3 and 4, respectively.

Arrays 2, 3, and 4 achieved comparable return loss responses to the free space for all five distances (Figure 33). The return loss curves are slightly shifted to the left of the free space. The VSWR curves at 4 mm away from the phantom are compared in Figure 34. The radiation patterns of both the E and H planes show reduced back radiation with more gratified lobes. The patterns improved and resembled the free space patterns at 10 mm for all three arrays. The patterns for all three arrays at 4 mm are compared in Figure 35. The

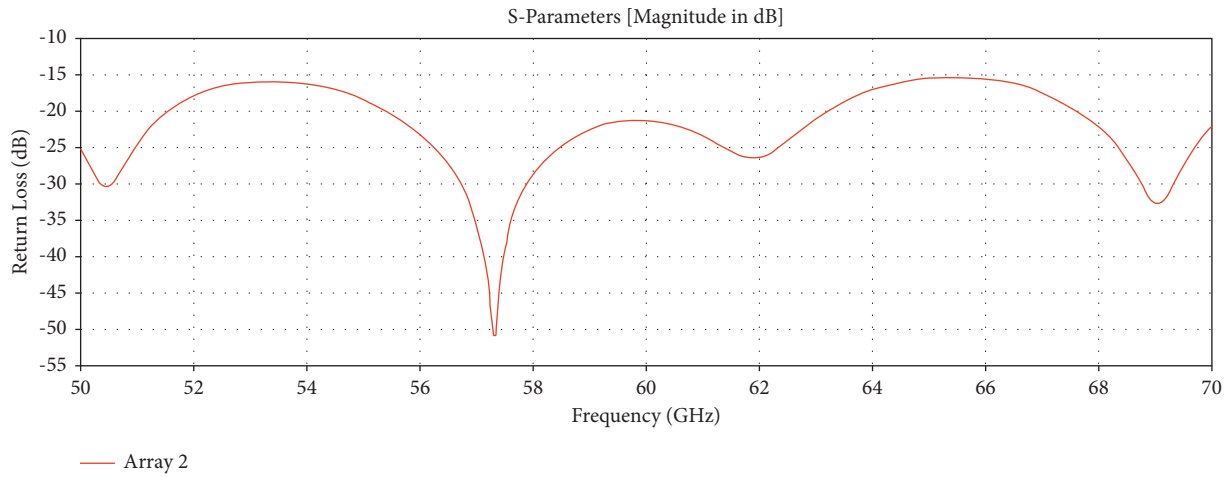


FIGURE 4: Simulated free-space return loss of Array 2.

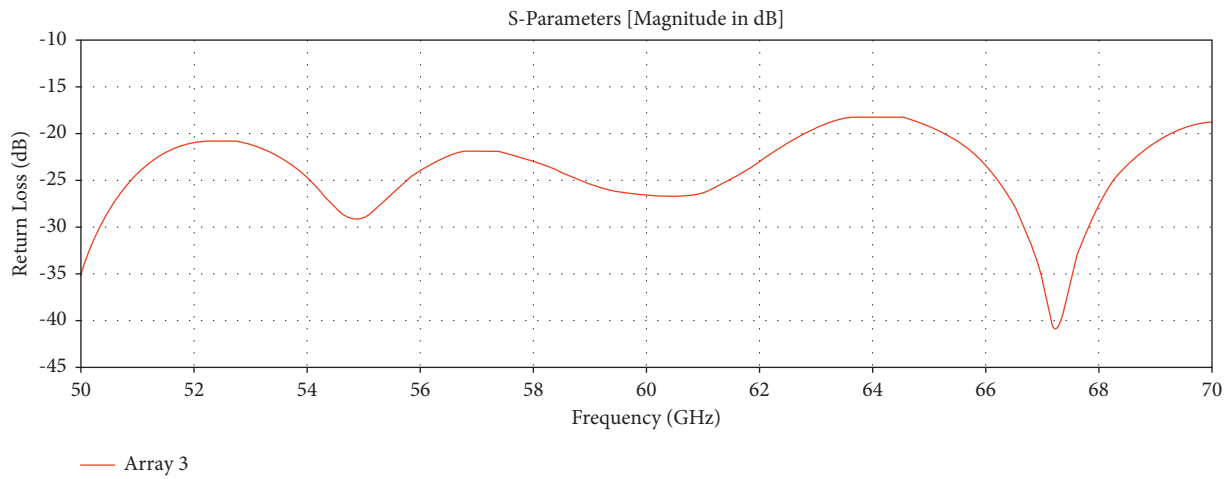


FIGURE 5: Simulated free-space return loss of Array 3.

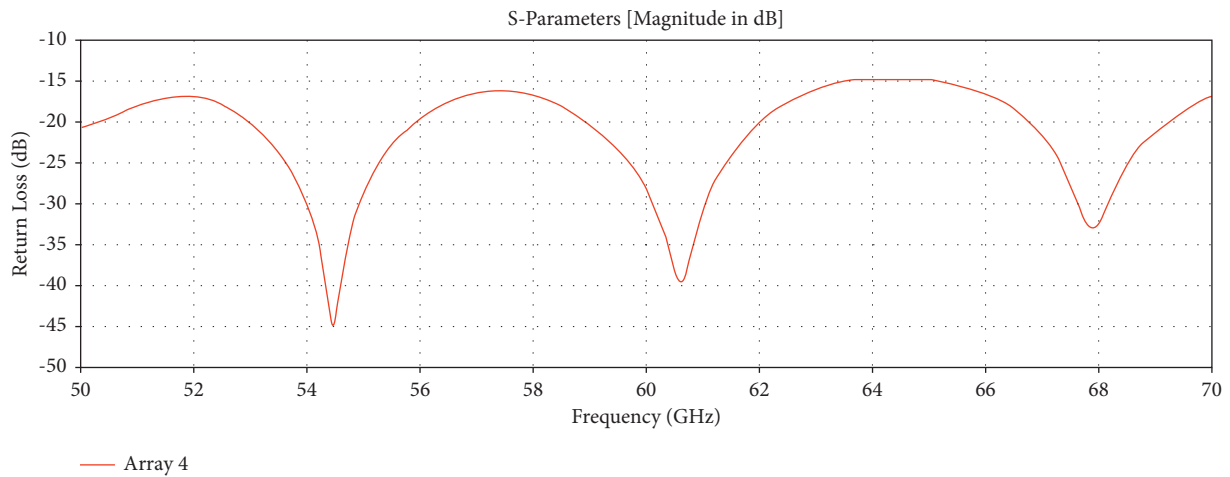


FIGURE 6: Simulated free-space return loss of Array 4.

radiation and total efficiency dropped significantly at 2 mm. These parameters improved gradually with an increase in the gap between the phantom and the antenna.

This study's results are compared to those of other articles in Table 11. In [10], a textile-based 60 GHz array antenna is presented. The antenna is designed on a cotton

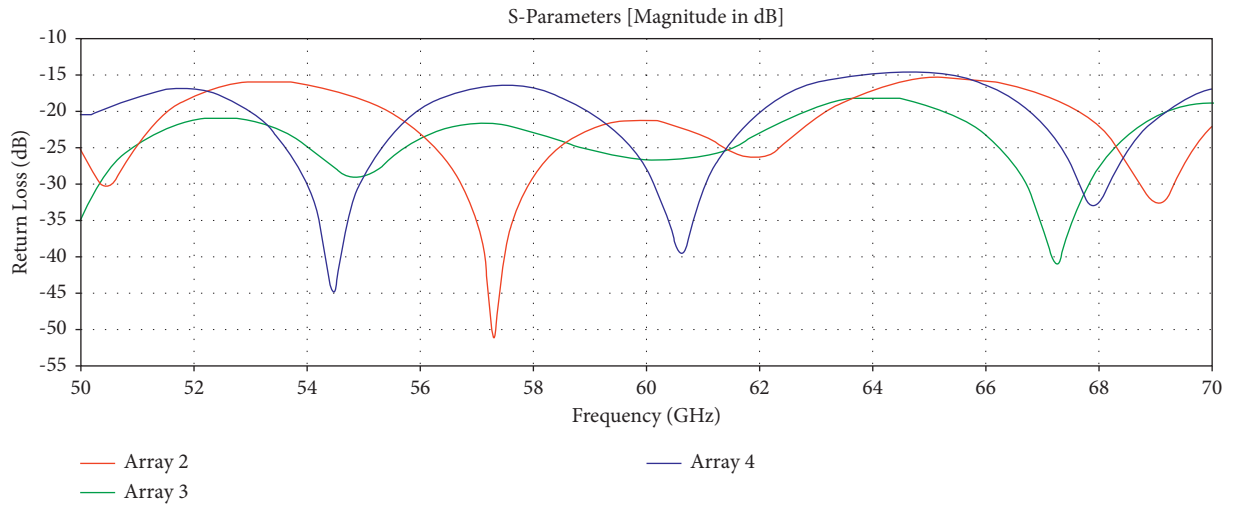


FIGURE 7: Simulated free-space return loss comparison.

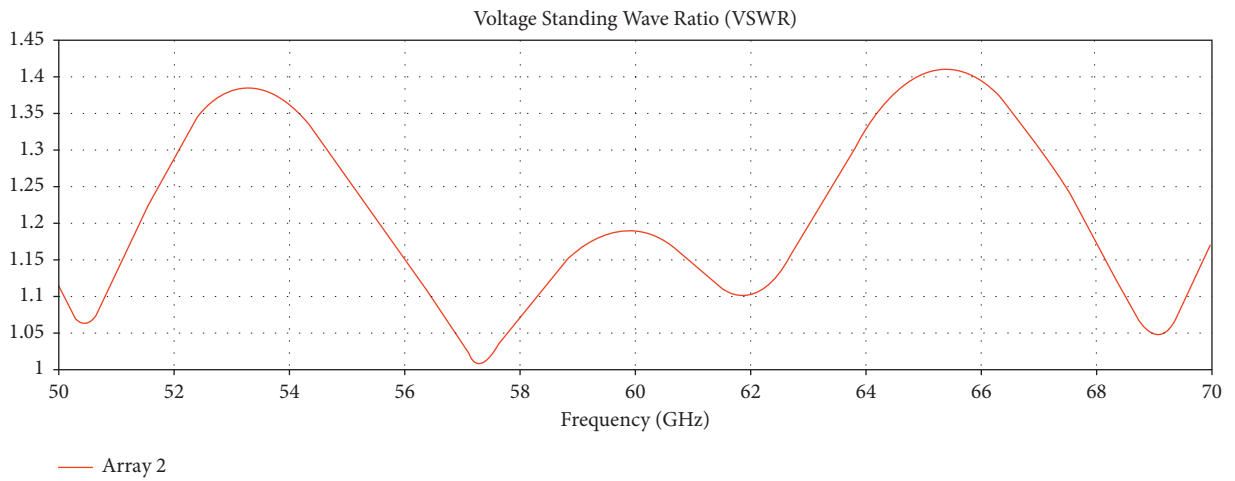


FIGURE 8: Free-space VSWR of Array 2.

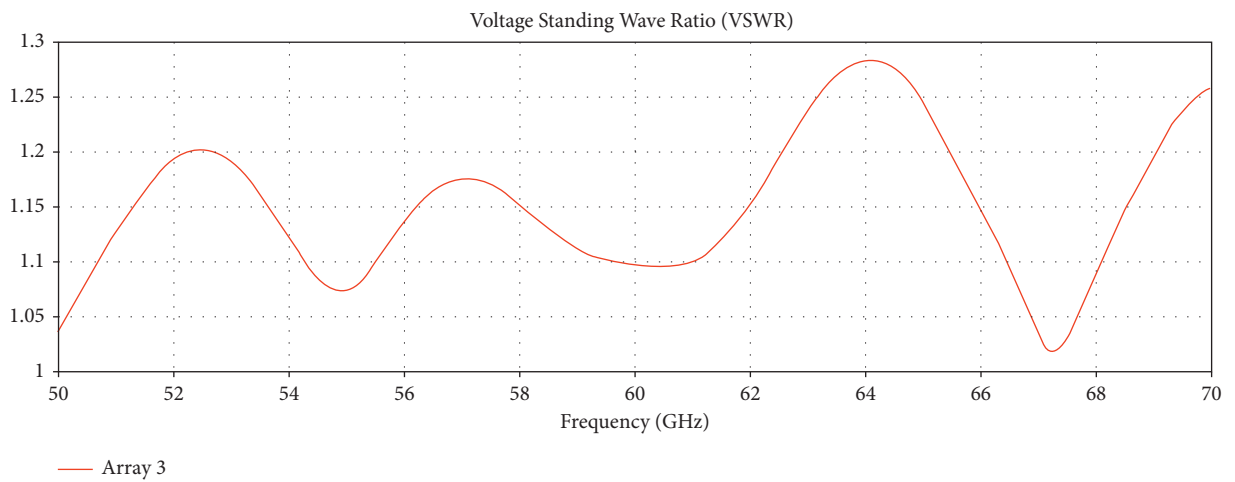


FIGURE 9: Free-space VSWR of Array 3.

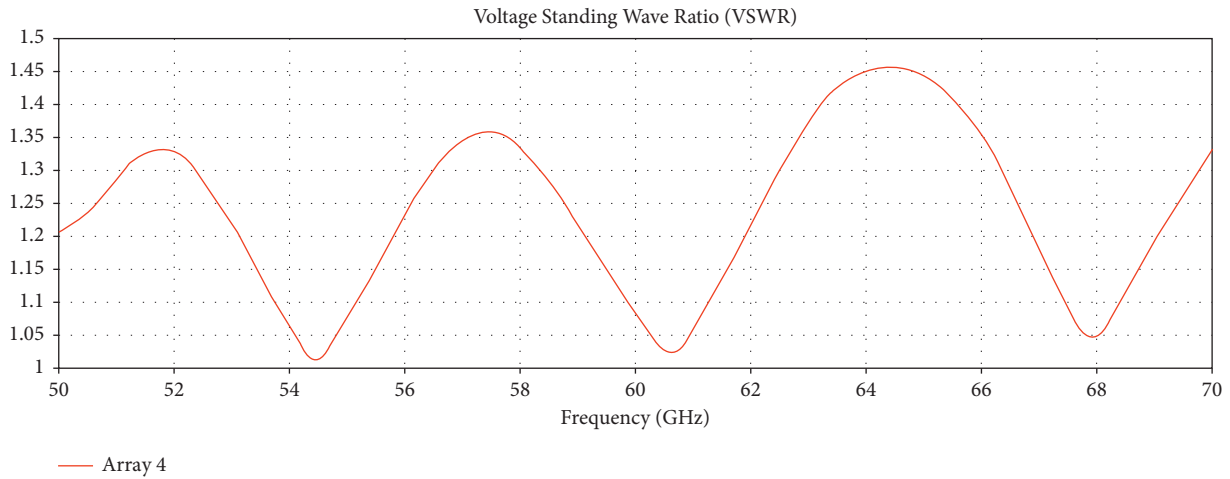


FIGURE 10: Free-space VSWR of Array 4.

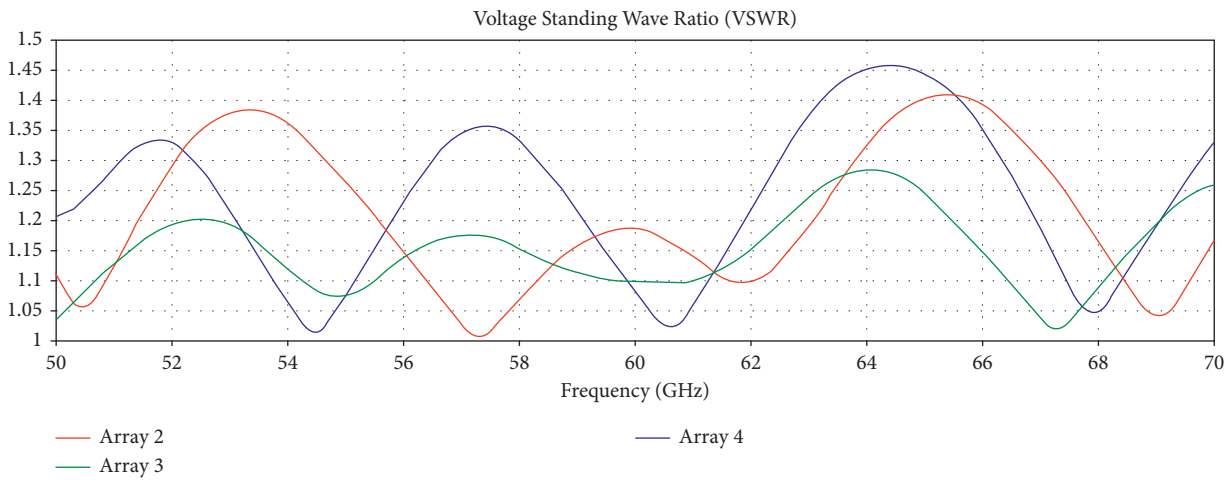


FIGURE 11: Free-space VSWR comparison.

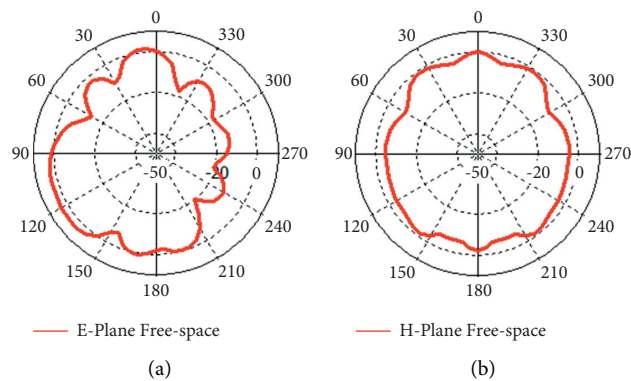


FIGURE 12: Radiation pattern of Array 2. (a) E-plane radiation pattern at 60 GHz. (b) H-plane radiation pattern at 60 GHz.

textile substrate. The overall size of the antenna is larger compared to the antenna presented in this study. A cotton-based Yagi-Udah antenna is presented by the same author in [18]. The antenna is also larger in size in comparison to the antenna presented in this study. In [23], a polyester-

based textile antenna is presented, which is not an array. The antenna presented in [24] is based on the FR-4 substrate and it is not an array antenna. The proposed antenna design in this study is an array antenna. It is more compact compared to other articles. The antenna in this study has a

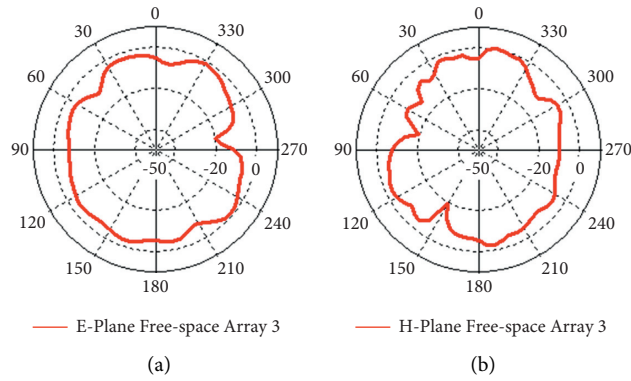


FIGURE 13: Radiation pattern of Array 3. (a) E-plane radiation pattern at 60 GHz. (b) H-plane radiation pattern at 60 GHz.

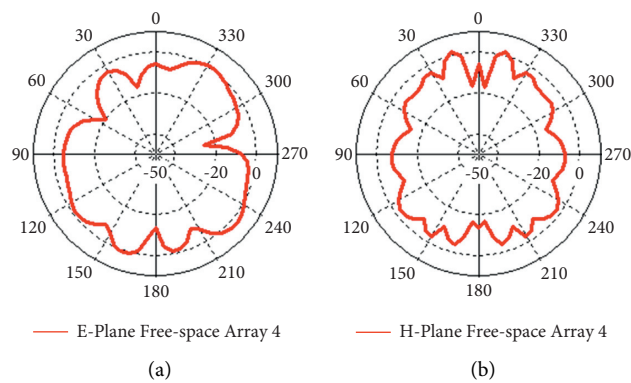


FIGURE 14: Radiation pattern of Array 4. (a) E-plane radiation pattern at 60 GHz. (b) H-plane radiation pattern at 60 GHz.

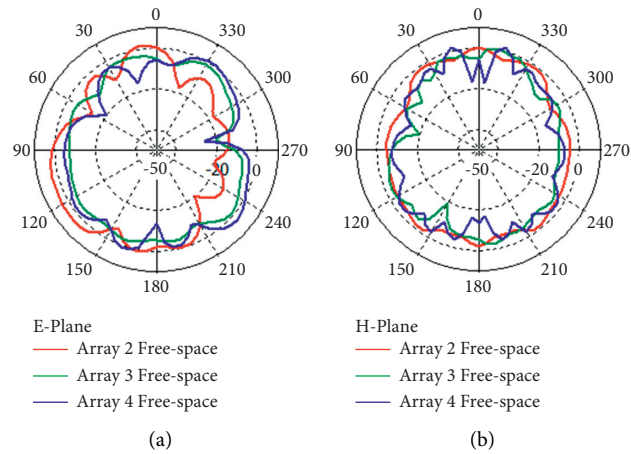


FIGURE 15: Radiation pattern comparison of Array 2, Array 3, and Array 4: (a) E-plane and (b) H-plane.

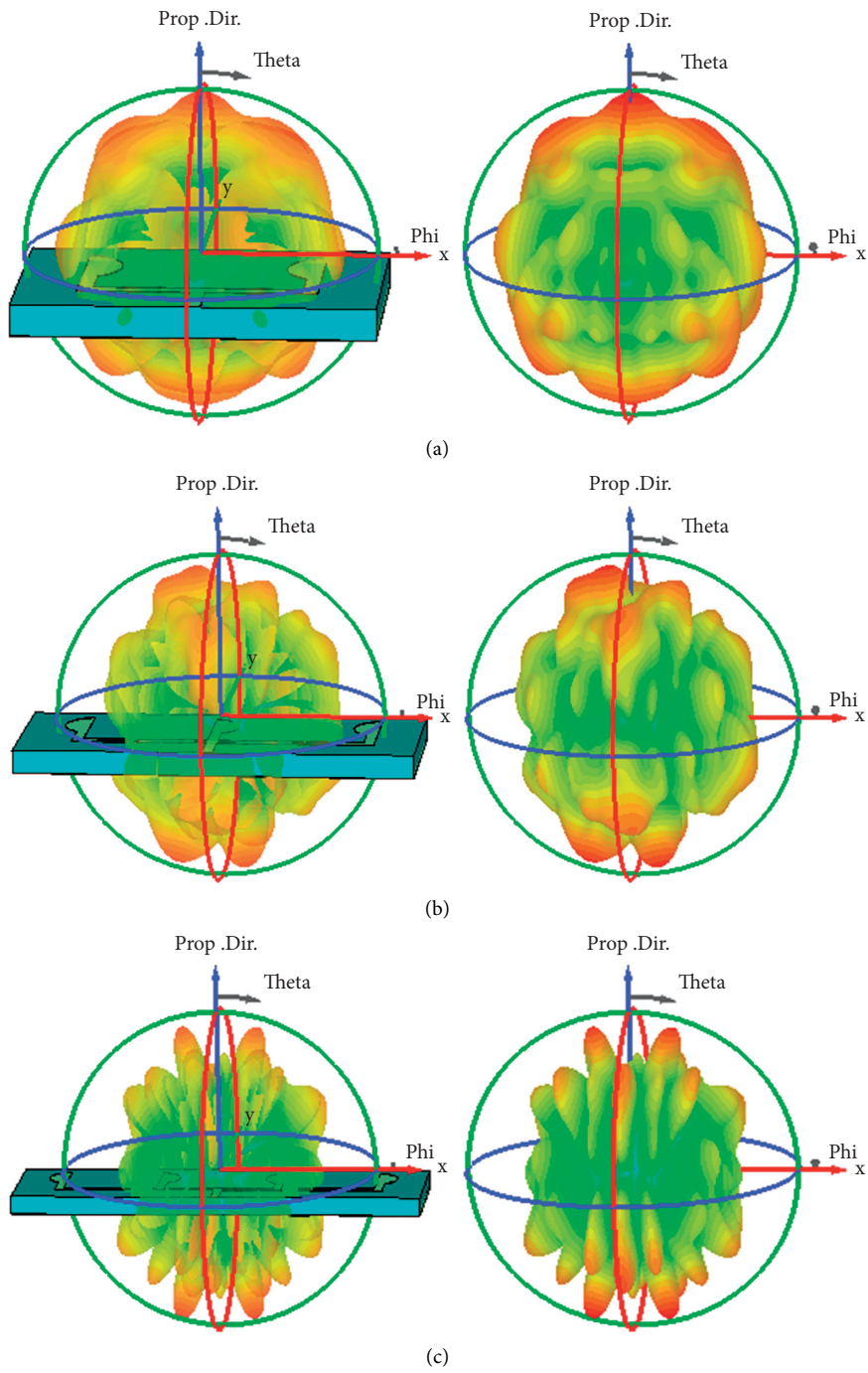


FIGURE 16: 3 Radiation with and without structure of (a) Array 2, (b) Array 3, and (c) Array 4.

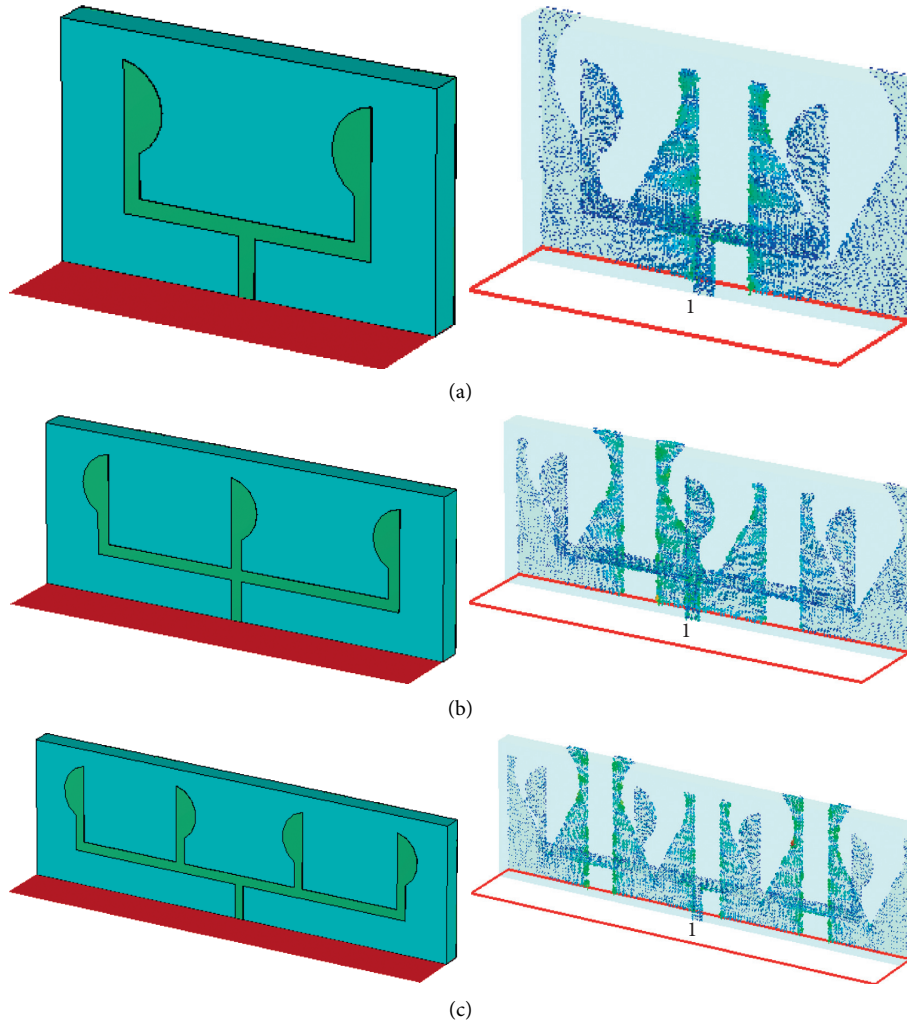


FIGURE 17: Surface current distribution of (a) Array 2, (b) Array 3, and (c) Array 4.

TABLE 5: Free-space array performance comparison.

Parameters at 60 GHz	Array 2	Array 3	Array 4
Return loss Magnitude (dB)	-21.264423	-26.629909	-28.015424
VSWR	1.189	1.098	1.0827
Gain (dBi)	3.436	4.292	6.195
Radiation efficiency (%)	41.51	32.64	33.61
Total efficiency (%)	41.20	32.57	33.56

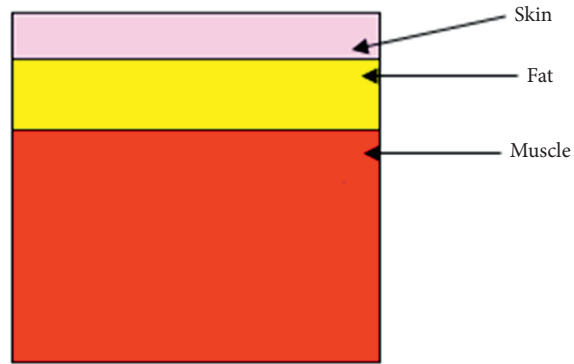


FIGURE 18: Phantom consisting of three outer most layer of human body.

TABLE 6: Dimension and physical properties of skin, fat, and muscle at 60 GHz [25].

Phantom layers	Thickness (mm)	Relative permittivity	Conductivity	Average penetration depth (mm)
Skin	2	7.98	36.39	0.48
Fat	3	3.13	2.82	3.37
Muscle	10	12.86	52.83	0.41

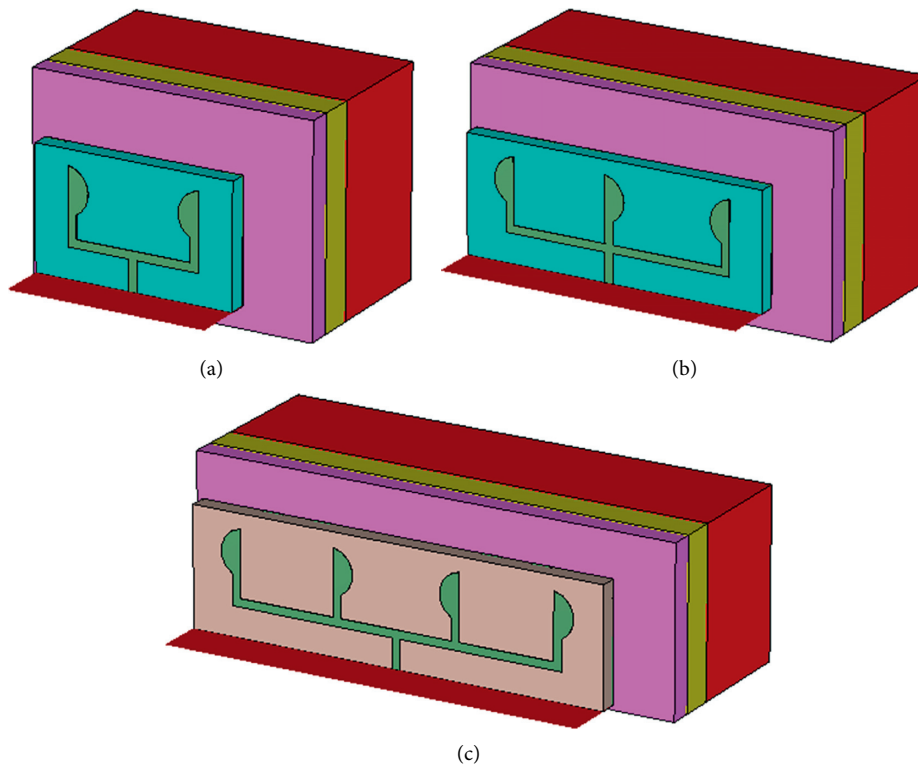


FIGURE 19: Array 2, 3, and 4 placed on top of the human phantom. (a) Array two. (b) Array three. (c) Array four.

TABLE 7: Phantom dimension for different array configuration.

Array design	Phantom dimension
Array 2	23.5 mm × 17 mm
Array 3	32 mm × 17 mm
Array 4	41.5 mm × 17 mm

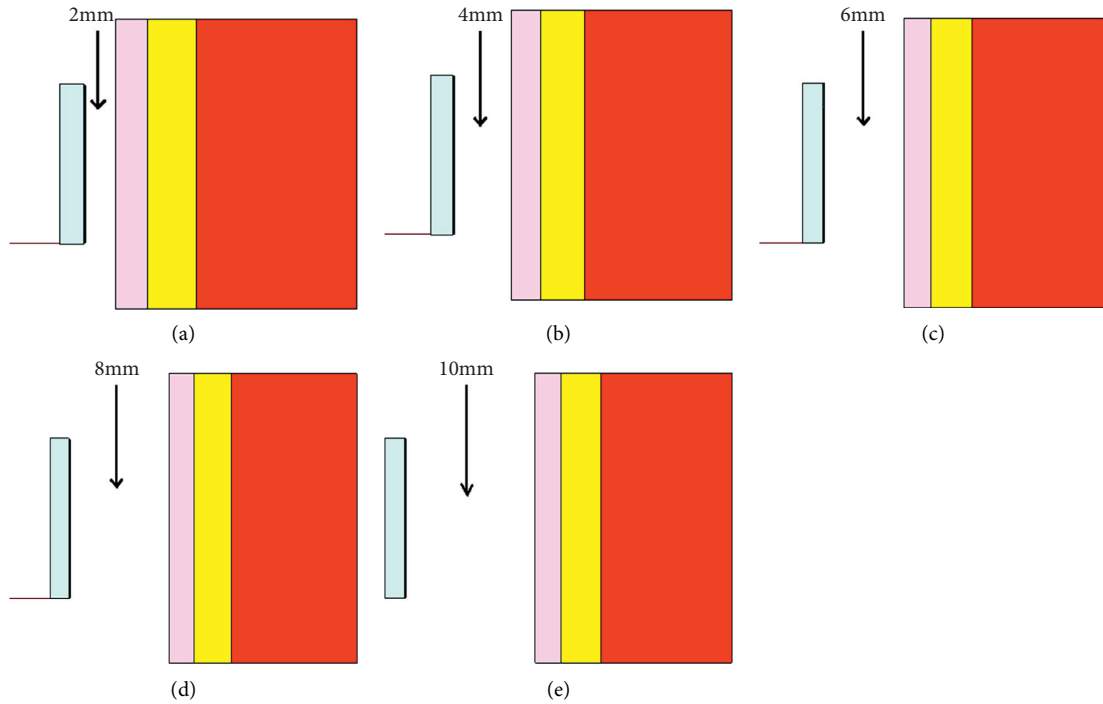


FIGURE 20: Arrays placed at 5 different distances away from phantom. (a) 2 mm. (b) 4 mm. (c) 6 mm. (d) 8 mm. (e) 10 mm.

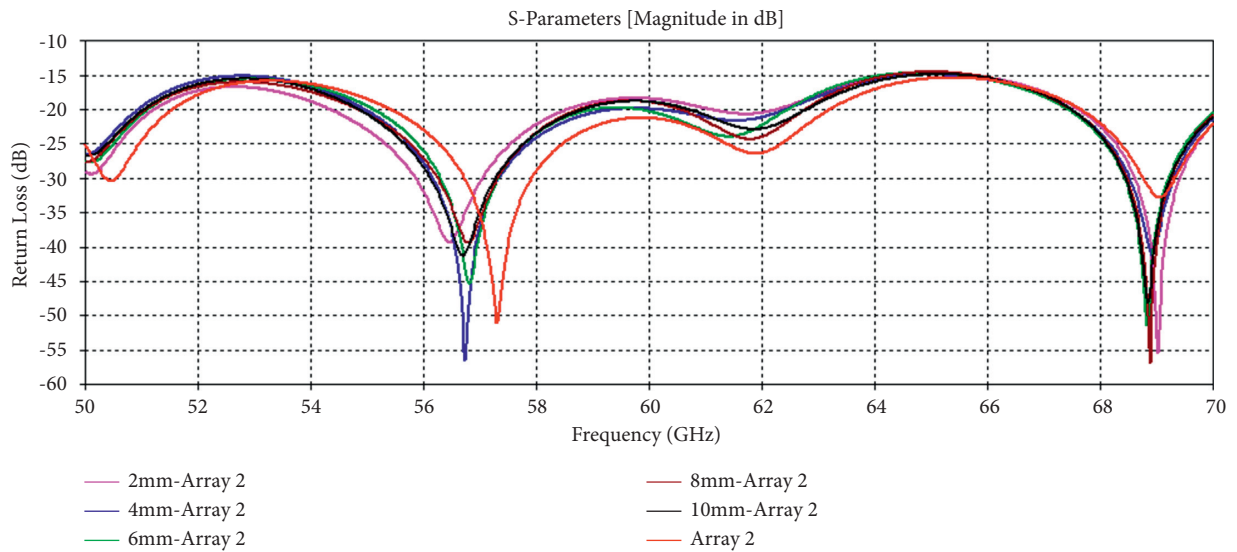


FIGURE 21: Simulated Array 2 on-body return loss at different distances compared to free space.

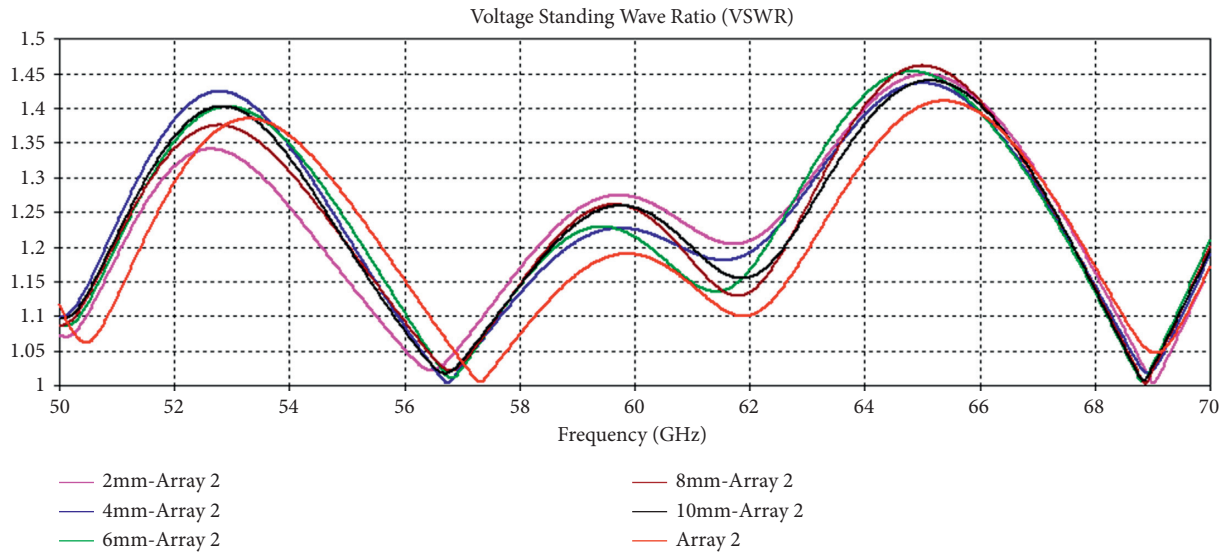


FIGURE 22: Array 2 on-body VSWR at different distances compared to free space.

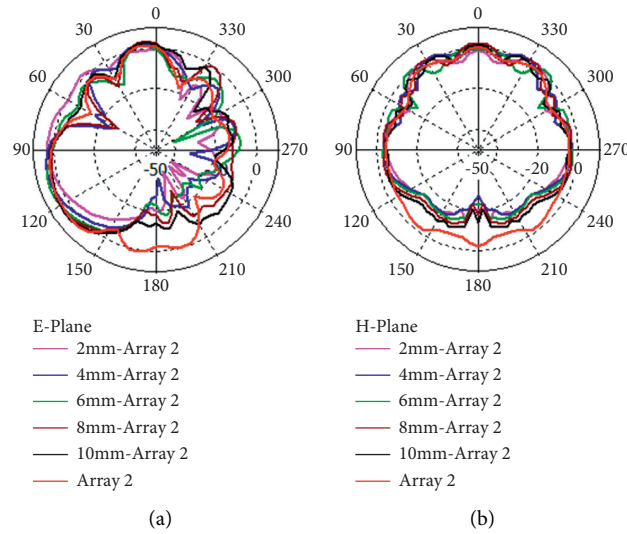


FIGURE 23: Array 2 on-body radiation pattern at 60 GHz. (a) E-plane. (b) H-plane.

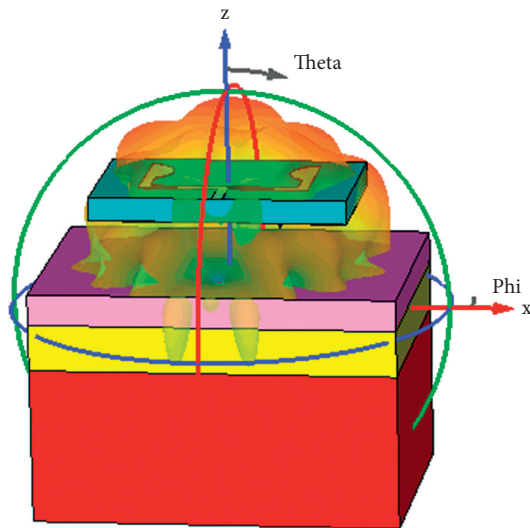


FIGURE 24: Array 2 on-body 3D radiation pattern at 60 GHz.

TABLE 8: Array 2 on-body results at different gap distances.

Parameters at 60 GHz	Free-space	On-body 2 mm	On-body 4 mm	On-body 6 mm	On-body 8 mm	On-body 10 mm
Return loss (dB)	-21.264	-18.450	-19.899	-20.279	-18.942	-18.883
VSWR	1.189	1.271	1.225	1.214	1.254	1.256
Gain (dBi)	3.436	3.381	4.464	4.855	4.375	4.243
Radiation efficiency (%)	41.51	29.49	33.19	34.97	36.87	38.52
Total efficiency (%)	41.20	29.07	32.85	34.64	36.40	38.02

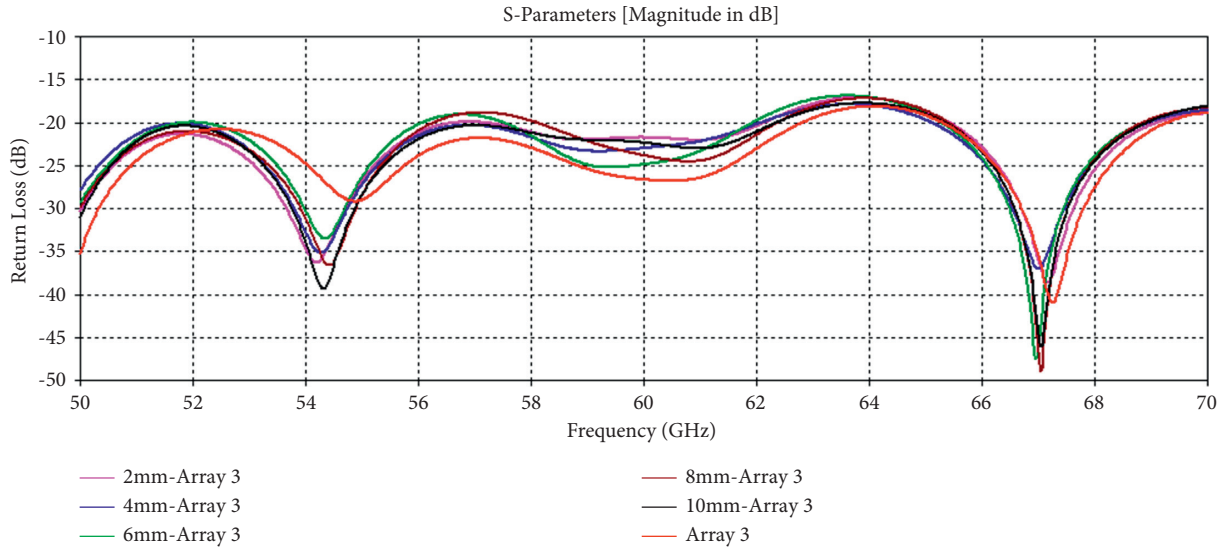


FIGURE 25: Simulated Array 3 on-body return loss at different distances compared to free space.

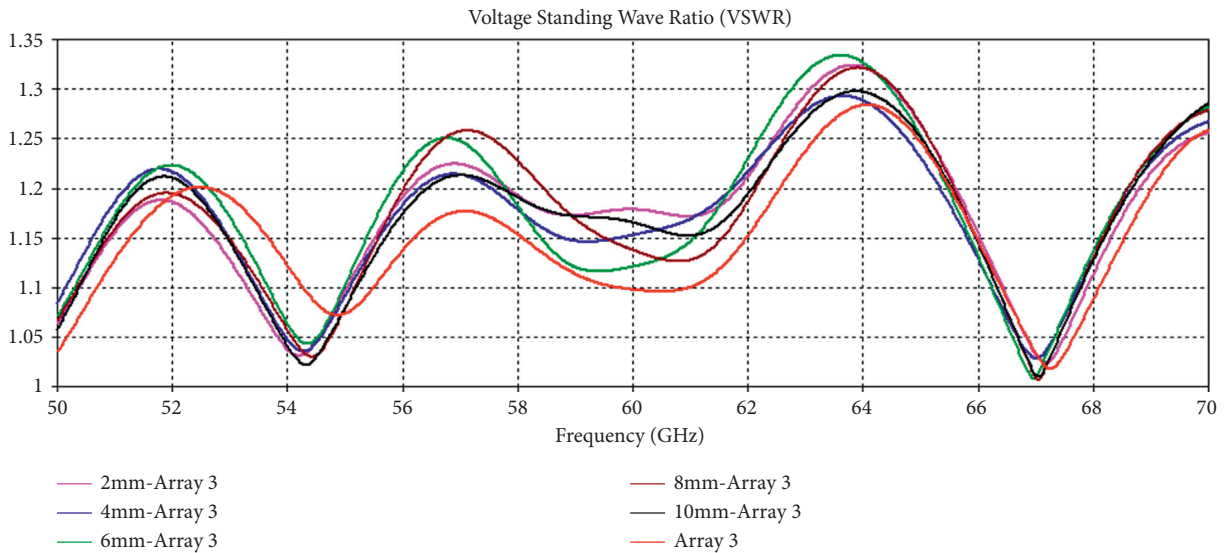


FIGURE 26: Array 3 on-body VSWR at different distances compared to free space.

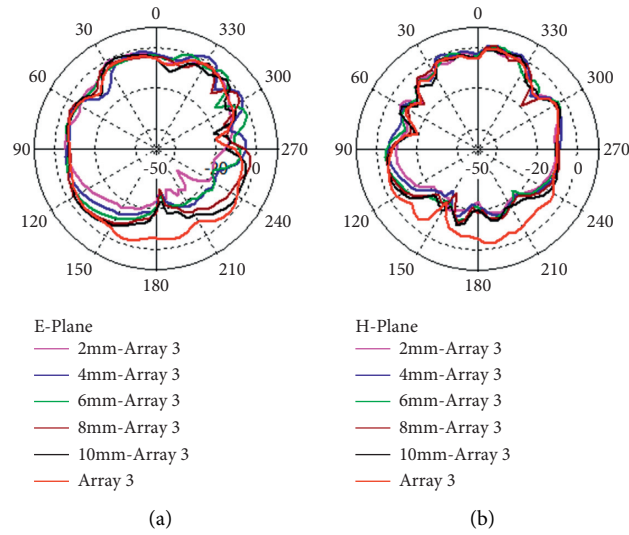


FIGURE 27: Array 3 on-body radiation pattern at 60 GHz. (a) E-plane. (b) H-plane.

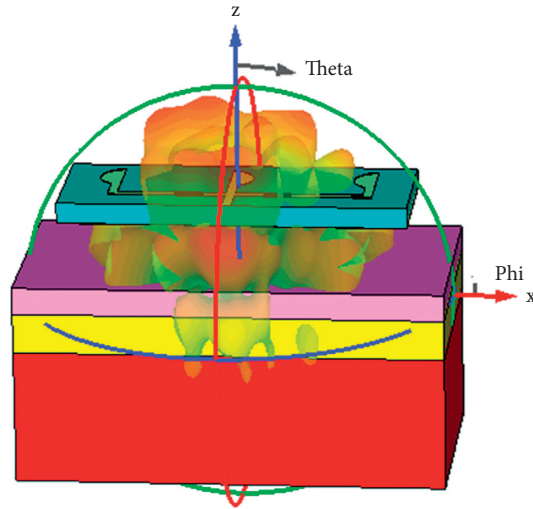


FIGURE 28: Array 3 on-body 3D radiation pattern at 60 GHz.

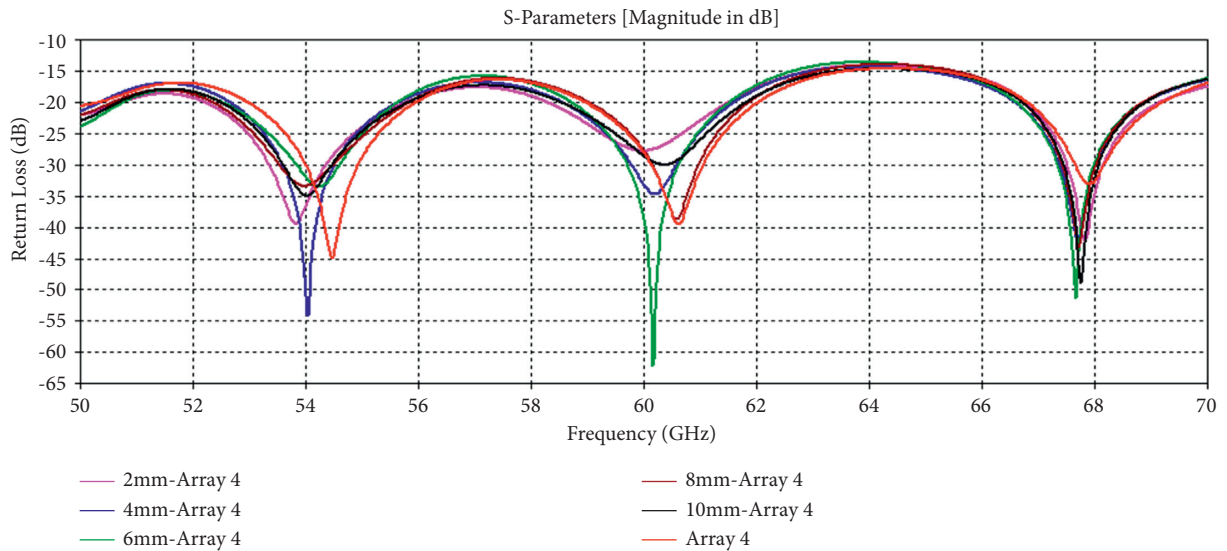


FIGURE 29: Simulated Array 4 on-body return loss at different distances compared to free space.

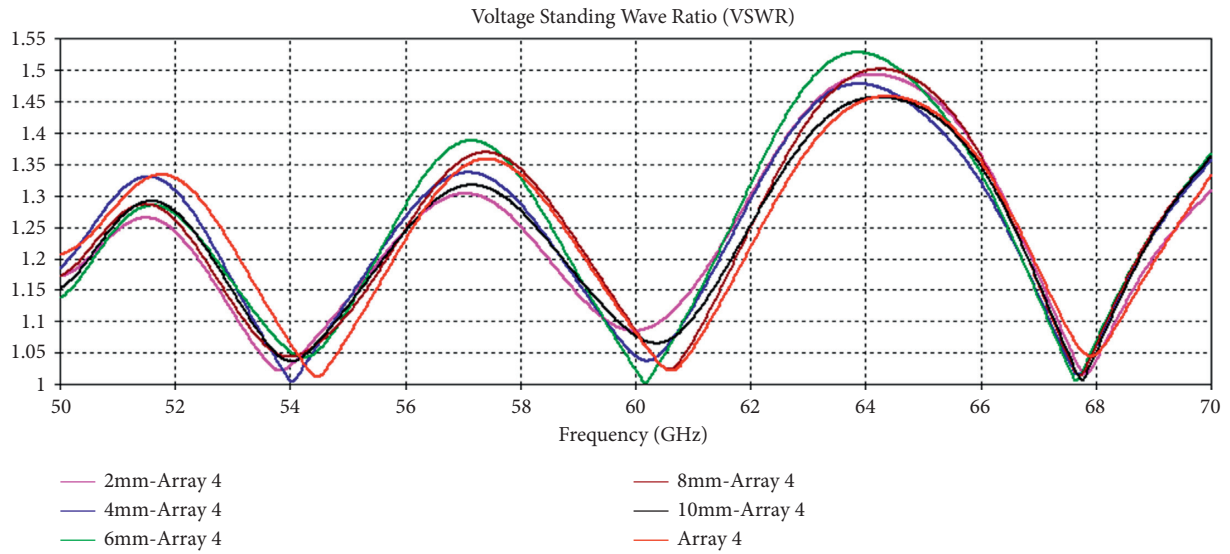


FIGURE 30: Array 4 on-body VSWR at different distances compared to free space.

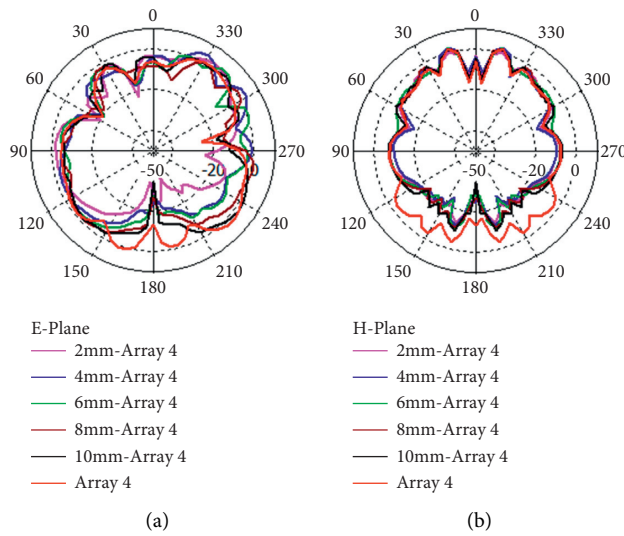


FIGURE 31: Array 4 on-body radiation pattern at 60 GHz. (a) E-plane. (b) H-plane.

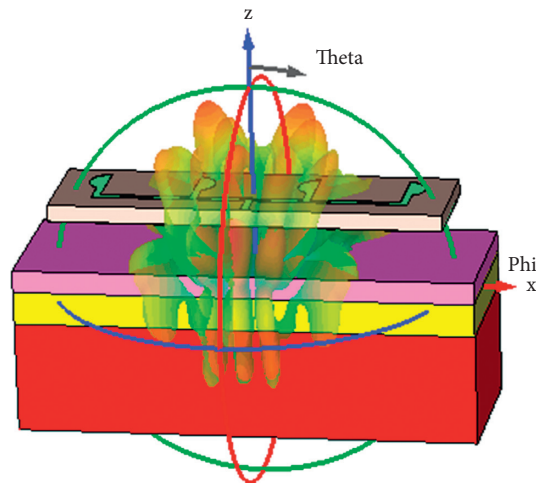


FIGURE 32: Array 4 on-body 3D radiation pattern at 60 GHz.

TABLE 9: Array 3 on-body results at different gap distances.

Parameters at 60 GHz	Free-space	On-body 2 mm	On-body 4 mm	On-body 6 mm	On-body 8 mm	On-body 10 mm
Return loss (dB)	-26.629	-21.725	-22.976	-24.877	-23.827	-22.336
VSWR	1.097	1.178	1.152	1.120	1.137	1.165
Gain (dBi)	4.292	3.238	4.622	5.032	4.947	4.987
Radiation efficiency (%)	32.64	23.52	26.59	28.11	28.62	29.90
Total efficiency (%)	32.57	23.36	26.46	28.01	28.50	29.73

TABLE 10: Array 4 on-body results at different gap distances.

Parameters at 60 GHz	Free-space	On-body 2 mm	On-body 4 mm	On-body 6 mm	On-body 8 mm	On-body 10 mm
Return loss (dB)	-28.015	-27.771	-33.152	-38.623	-27.701	-28.568
VSWR	1.082	1.085	1.044	1.023	1.085	1.077
Gain (dBi)	6.195	5.960	6.665	6.395	6.411	6.140
Radiation efficiency (%)	33.61	24.76	26.86	27.87	28.50	29.90
Total efficiency (%)	33.56	24.72	26.85	27.87	28.45	29.86

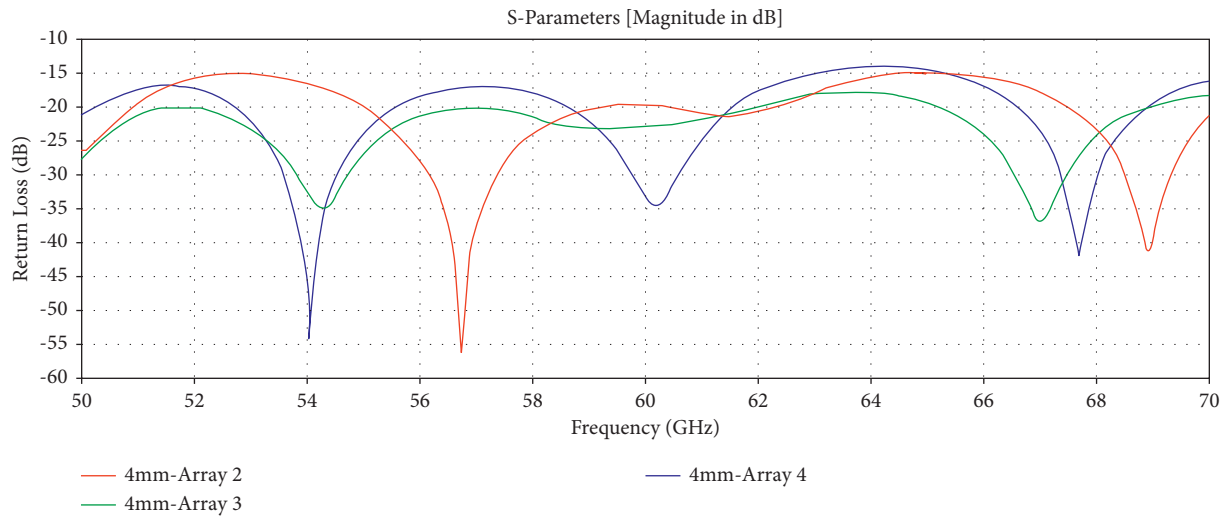


FIGURE 33: On-body return loss comparison at 4 mm between Array 2, 3, and 4.

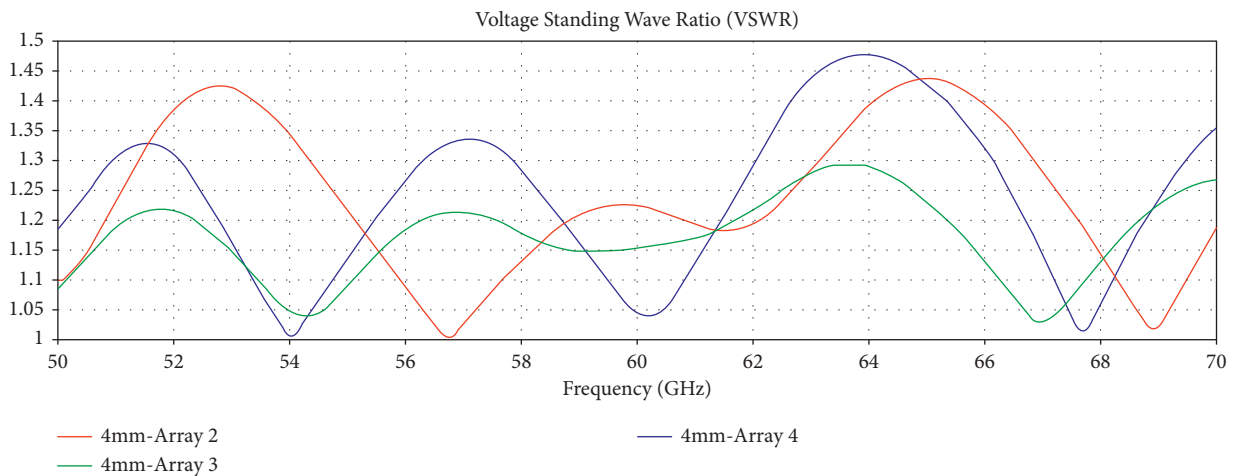


FIGURE 34: On-body VSWR comparison at 4 mm between Array 2, 3, and 4.

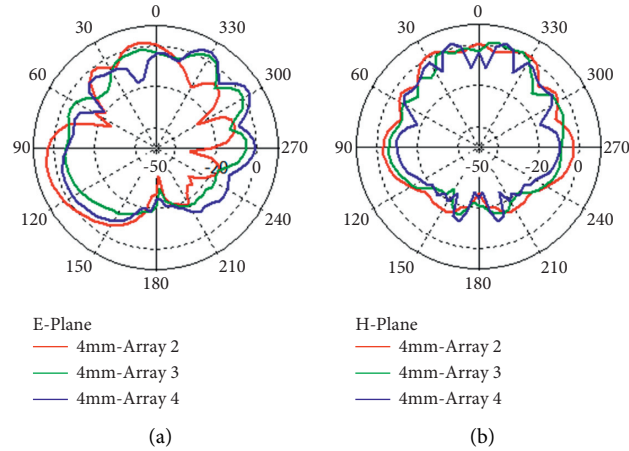


FIGURE 35: 60 GHz on-body comparison of radiation patterns between Array 2, 3, and 4. (a) E-plane. (b) H-plane.

TABLE 11: A comparison of this paper's research with that of other articles.

Antenna	Size length (L) and width (W) mm	Relative permittivity	Substrate	Bandwidth (GHz) at -10 dB	Gain (dBi)	Efficiency (%)	Antenna category
Ref [10]	50 × *	2	Cotton	55–65	8.6	41	Array
Ref [18]	26 × 8	1.5	Cotton	57–64	9	74	Yagi-Uda
Ref [23]	12.2 × 12	1.9	100% polyester	11.632	5.96	58.03	Slotted patch
Ref [24]	12.9 × 14	4.3	FR-4	12.11	8.62	82.15	Q-slot
This paper 2 array	10 × 16.5	4.3	FR-4	More than 20 GHz	3.436	41.51	Array 2
This paper 3 array	10 × 26	4.3	FR-4	More than 20 GHz	4.292	32.64	Array 3
This paper 4 array	10 × 35.5	4.3	FR-4	More than 20 GHz	6.195	33.61	Array 4

*Exact value not provided.

very wide bandwidth compared to the other antennas in the literature.

5. Conclusion

In this paper, we have presented three different arrays of a 60 GHz super-wideband antenna. Due to a lack of adequate facilities, no measurements were conducted, so we only provided simulated findings. The CST simulation results are reliable, and we expect any future measurements taken will be within the margin of error. Arrays are designed to achieve high gain, which is required to increase the range at 60 GHz. The gain increased as the number of elements increased, but not at the same rate as in other reported works. The maximum gain achieved by all three arrays is suitable for very short-range communication. Efficiency was also affected, especially under on-body scenarios. Microstrip patch antennas usually have low efficiency, low bandwidth, and a broadside radiation pattern. Results presented in this paper confirm this, even though we managed to achieve high bandwidth. On-body applications require broadside radiation, which is achieved by these arrays. The antenna designs presented in this paper are

very small, and thus careful fabrication is required to take performance measurements. The proposed antenna in this study is novel compared to the presented antennas in the open literature. This structure of the antenna is new and is a compact array antenna for body-centric communications (BCCs). It is a more compact antenna compared to the array antennas proposed for BCCs in other articles. Although the size of this presented array antenna is smaller, it shows a huge bandwidth of more than 20 GHz. The gain of the antenna increases as the number of antenna arrays is increased. The presented antenna shows more than 6 dBi gain. This antenna shows very good on-body performance. This study and the findings in this paper are comprehensive.

Data Availability

The data used to support the findings of this study are freely available at <http://niremf.ifac.cnr.it/tissprop/>.

Conflicts of Interest

The authors declare that they have no conflicts of interest.

Acknowledgments

The authors extend their appreciation to the Deanship of Scientific Research at King Khalid University for supporting this research through a Research Groups Program under Grant (RGP.1/49/42). The authors would also like to thank the support from the Taif University Researchers Supporting Project (TURSP-2020/26), Taif University, Taif, Saudi Arabia.

References

- [1] A. R. Guraliuc, M. Zhadobov, G. Valerio, N. Chahat, and R. Sauleau, "Effect of textile on the propagation along the body at 60 GHz," *IEEE Transactions on Antennas and Propagation*, vol. 62, no. 3, pp. 1489–1494, 2014.
- [2] A. R. Guraliuc, M. Zhadobov, G. Valerio, and R. Sauleau, "Enhancement of on-body propagation at 60 GHz using electro textiles," *IEEE Antennas and Wireless Propagation Letters*, vol. 13, pp. 603–606, 2014.
- [3] G. Chittimoju and U. Devi Yalavarthi, "A comprehensive review on millimeter waves applications and antennas," *Journal of Physics: Conference Series*, vol. 1804, no. 1, Article ID 012205, 2021.
- [4] M. García Sánchez, "Millimeter-wave communications," *Electronics*, vol. 9, no. 2, p. 251, 2020.
- [5] J. F. Harvey, M. B. Steer, and T. S. Rappaport, "Exploiting high millimeter wave bands for military communications, applications, and design," *IEEE Access*, vol. 7, pp. 52350–52359, 2019.
- [6] N. Chahat, G. Valerio, M. Zhadobov, and R. Sauleau, "On-body propagation at 60 GHz," *IEEE Transactions on Antennas and Propagation*, vol. 61, no. 4, pp. 1876–1888, 2013.
- [7] N. Chahat, M. Zhadobov, and R. Sauleau, "Broadband tissue-equivalent phantom for BAN applications at millimeter waves," *IEEE Transactions on Microwave Theory and Techniques*, vol. 60, no. 7, pp. 2259–2266, 2012.
- [8] R. Wu, H. Tang, K. Wang, C. Yu, J. Zhang, and X. Wang, "E-shaped array antenna with high gain and low profile for 60 GHz applications," in *Proceedings of the IEEE MTT-S International Microwave Workshop Series on Advanced Materials and Processes for RF and THz Applications (IMWS-AMP)*, pp. 1–3, Chengdu, China, 2016.
- [9] J. Puskely, M. Pokorny, J. Lacik, and Z. Raida, "Wearable disc-like antenna for body-centric communications at 61 GHz," *IEEE Antennas and Wireless Propagation Letters*, vol. 14, pp. 1490–1493, 2015.
- [10] N. Chahat, M. Zhadobov, L. Le Coq, and R. Sauleau, "Wearable endfire textile antenna for on-body communications at 60 GHz," *IEEE Antennas and Wireless Propagation Letters*, vol. 11, pp. 799–802, 2012.
- [11] K. Islam, T. Hossain, and M. M. Khan, "A compact novel design of a 60 GHz antenna for body-centric communication," *International Journal on Communications Antenna and Propagation (IRECAP)*, vol. 10, no. 5, pp. 325–333, 2020.
- [12] K. Islam, T. Hossain, M. Monirujjaman Khan, M. Masud, and R. Alroobaea, "Comparative design and study of a 60 GHz antenna for body-centric wireless communications," *Computer Systems Science and Engineering*, vol. 37, no. 1, pp. 19–32, 2021.
- [13] J. Jichao Zhan, J. Jincai Wen, L. Xiongjun Shu, and X. Shu, "Design of 60 GHz mm-wave patch antenna arrays," in *Proceedings of the 2015 IEEE 16th International Conference on Communication Technology (ICCT)*, pp. 262–265, Hangzhou, China, 2015.
- [14] B. Lu, J. Luo, R. Yue, and Y. Wang, "A Yagi antenna array for 60-GHz WPAN," in *Proceedings of the 2011 IEEE International Conference of Electron Devices and Solid-State Circuits*, pp. 1–2, Tianjin, China, 2011.
- [15] J. Li and N. Ghalichechian, "A high-gain large-scanning 60 GHz via-fed patch phased array antenna," in *Proceedings of the 2018 IEEE International Symposium on Antennas and Propagation & USNC/URSI National Radio Science Meeting*, pp. 1701–1702, Boston, MA, USA, 2018.
- [16] W. Yang, K. Ma, K. S. Yeo, and W. M. Lim, "A compact high-performance patch antenna array for 60-GHz applications," *IEEE Antennas and Wireless Propagation Letters*, vol. 15, pp. 313–316, 2016.
- [17] Y. Hong and J. Choi, "60-GHz array antenna for mm-wave 5G wearable applications," in *Proceedings of the 2018 IEEE International Symposium on Antennas and Propagation & USNC/URSI National Radio Science Meeting*, pp. 1207–1208, Boston, MA, USA, 2018.
- [18] N. Chahat, M. Zhadobov, S. A. Muhammad, L. Le Coq, and R. Sauleau, "60-GHz textile antenna array for body-centric communications," *IEEE Transactions on Antennas and Propagation*, vol. 61, no. 4, pp. 1816–1824, 2013.
- [19] N. Chahat, M. Zhadobov, L. Le Coq, S. I. Alekseev, and R. Sauleau, "Characterization of the interactions between a 60-GHz antenna and the human body in an off-body scenario," *IEEE Transactions on Antennas and Propagation*, vol. 60, no. 12, pp. 5958–5965, 2012.
- [20] C. Leduc and M. Zhadobov, "Impact of antenna topology and feeding technique on coupling with human body: application to 60-GHz antenna arrays," *IEEE Transactions on Antennas and Propagation*, vol. 65, no. 12, pp. 6779–6787, 2017.
- [21] X. Y. Wu, L. Akhoondzadeh-Asl, Z. P. Wang, and P. S. Hall, "Novel Yagi-Uda antennas for on-body communication at 60 GHz," in *Proceedings of the Loughborough Antennas & Propagation Conference*, pp. 153–156, Loughborough, UK, 2010.
- [22] S. H. Kiani, X. C. Ren, A. Bashir et al., "Square-framed T shape mmwave antenna array at 28 GHz for future 5G devices," *International Journal of Antennas and Propagation*, vol. 2021, no. 2286011, pp. 1–9, 2021.
- [23] M. Monirujjaman Khan, K. Islam, M. N. A. Shovon, M. Masud, M. Baz, and M. A. AlZain, "Various textiles-based comparative analysis of a millimeter wave miniaturized novel antenna design for body-centric communications," *International Journal of Antennas and Propagation*, vol. 2021, Article ID 2360440, 14 pages, 2021.
- [24] M. M. Khan, K. Islam, and N. A. Shovon, "Design of a novel 60 GHz millimeter wave Q-slot antenna for body-centric communications," *International Journal of Antennas and Propagation*, vol. 2021, Article ID 9795959, 12 pages, 2021.
- [25] D. Andreuccetti, *Dielectric Properties of Body Tissues in the Frequency Range 10 Hz to 100 GHz*, Italian National Research Council, Rome, Italy, 2021, [Online]. Available: <http://niremf.ifac.cnr.it/tissprop/>.